GEOMETRICALLY NONLINEAR FINITE ELEMENT ANALYSIS OF SPACE FRAMES

Alysson B. Barros[1], Jordlly R. B. Silva[2], Felipi P. D. Fernandes[1]

[1]*Federal Rural University of Pernambuco, Academic Unit of Cabo de Santo Agostinho (UFRPE/UACSA)*
Rua. Cento e Sessenta e Três, 300, 54518-430, Cabo de Santo Agostinho/PE, Brazil
alysson.barbosa@ufrpe.br, felipi.fernandes@ufrpe.br
[2]*Dept. of Civil and Environmental Engineering, Federal University of Pernambuco (UFPE)*
Av. Prof. Moraes Rego, 1235, 50670-901, Recife/PE, Brazil
jordlly.silva@ufpe.br

Abstract. In structural engineering, the von Kármán theory provides a robust framework for modeling geometric nonlinearity under moderate displacements while assuming small strains, making it adequate for thin-walled structures and slender frames. This work presents a Python-based finite element method (FEM) program for nonlinear analysis of space frames, implementing the von Kármán hypothesis for beams. An arc-length scheme solves the nonlinear equilibrium equations. Post-processing via PyVista and Matplotlib libraries enables intuitive interpretation of deformed configuration and force distributions. The program was validated using Abaqus and RFEM, comparing both displacements and internal forces. An eigenvalue buckling analysis module was also implemented, yielding results within 1.5% of Abaqus in complex scenarios and matching exactly those from RFEM. The source code is openly available on GitLab under the name SimuFrame, providing full access to all modules and examples. Its applications are relevant to civil engineering, especially in designs considering the second-order effects.

Keywords: finite element method, geometric nonlinearity, von Kármán theory, structural engineering, python.

1 Introduction

Many scientific fields rely on linear models for analytical solutions. However, in structural engineering, material properties and large displacements often lead to nonlinear behavior, making exact solutions impractical. This complexity motivates the use of numerical methods such as the Finite Element Method (FEM), which became feasible with computers in the mid-20th century, as discussed by Lotti et al. [1], Vaz [2] and Zienkiewicz [3].

FEM is a numerical technique that involves discretizing a continuous domain into finite elements, each governed by the same differential equations, as stated by Lotti et al. [1]. In structural analysis, these equations yield parameters such as stress, strain, displacements, and internal forces.

Depending on the nature of the loading and deformation, structural analysis can be either linear or nonlinear. In linear analysis, equilibrium is evaluated in the undeformed configuration, assuming a proportional relationship between loads and displacements, according to Foletto et al. [4]. This work, however, focuses solely on geometric nonlinearity, disregarding the effects of material nonlinearity. The material is assumed to remain elastic, but equilibrium considers the deformed configuration, leading to a nonlinear strain–displacement relationship.

To capture this behavior, the von Kármán plate theory was adapted for beam elements, assuming that: (a) the height h is much smaller than the beam length L; (b) the deflections are of the same order as h; (c) the slopes are small, i.e. $|\partial w/\partial x| \ll 1$ and $|\partial w/\partial y| \ll 1$; (d) the tangential displacements v and w are small, and only the nonlinear terms involving $\partial v/\partial x$ and $\partial w/\partial y$ are retained; and (e) all strain components remain small, according to Figueiras [5]. This work, however, adopts a more general formulation by retaining all nonlinear terms, thereby accounting for the complete quadratic contributions.

2 Interpolation functions

The discrete model approximates the continuous behavior of a frame element. The discrete solution is defined by nodal displacements, while the continuous response along the element is obtained through interpolation using shape functions [2]. Figure 1 shows the end displacements and forces of a von Kármán frame element.

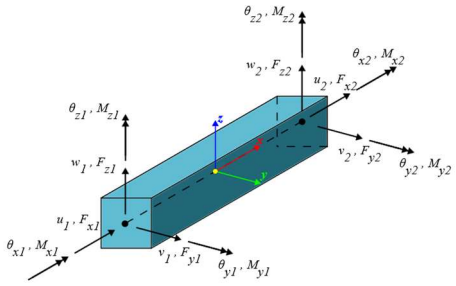


Figure 1. Displacement field of a space von Kármán frame element

In the axial direction, both the translational and the rotational displacement fields are approximated by a linear interpolation, whereas the transverse displacement field is represented by a cubic interpolation to adequately capture its higher-order deformation behavior. Based on the boundary conditions in Figure 1, the displacement fields are expressed in terms of shape functions, N:

$$u(x) = N_u^1 u_1 + N_u^2 u_2. \tag{1}$$

$$v(x) = N_v^1 v_1 + N_v^2 \theta_{z1} + N_v^3 v_2 + N_v^4 \theta_{z2}. \tag{2}$$

$$\theta_z(x) = N_{\theta_z}^1 v_1 + N_{\theta_z}^2 \theta_{z1} + N_{\theta_z}^3 v_2 + N_{\theta_z}^4 \theta_{z2}. \tag{3}$$

$$\theta_x(x) = N_{\theta_x}^1 \theta_{x_1} + N_{\theta_x}^2 \theta_{x_2}. \tag{4}$$

For the *x*-*z* plane, equivalent equations are derived by substituting $v \to w$ and $\theta_z \to \theta_y$. It is notable that the kinematic relationship is governed by the shape function matrix, $[N]$, and the nodal displacement vector, $\{d\}$:

$$\{U\}_{6x1} = [N]_{6x12}\{d\}_{12x1}. \tag{5}$$

3 Discretized frame model

The displacement field is defined according to the Euler–Bernoulli Beam Theory (EBBT), assuming that cross-sections remain plane and perpendicular to the neutral axis after deformation. Considering displacements in both *x*-*y* and *x*-*z* planes, and neglecting warping effects, the total displacement field is expressed as:

$$u(x,y,z) = u_0(x) - y\frac{\partial v(x)}{\partial x} + z\frac{\partial w(x)}{\partial x},\ v(x,y) = v_0(x),\ w(x,z) = w_0(x). \tag{6}$$

The nonlinear formulation accounts for second-order strain effects through the Green–Lagrange strain tensor, as shown in Rodrigues et al. [6]. Under von Kármán assumptions, the axial strain is expressed as the sum of a linear and a quadratic nonlinear term, capturing the coupling between axial stretching and transverse bending displacements, which are given by:

$$\varepsilon_{xx} = u_x + \frac{1}{2}(u_x^2 + v_x^2 + w_x^2). \tag{7}$$

Expanding using eq. (6):

$$\varepsilon_{xx} = \frac{\partial u_0(x)}{\partial x} - y\frac{\partial^2 v(x)}{\partial x^2} + z\frac{\partial w^2(x)}{\partial x^2} + \frac{1}{2}\left(\left(\frac{\partial u}{\partial x}\right)^2 + \left(\frac{\partial v}{\partial x}\right)^2 + \left(\frac{\partial w}{\partial x}\right)^2\right). \tag{8}$$

The transverse shear strains (γ_{xy}, γ_{xz}) are neglected, as the EBBT formulation does not account for shear deformation effects. By relating strains to displacements through the strain–displacement matrix $[B]$, eq. (8) can be rewritten as:

$$\{\varepsilon\} = [B]\{d\} = \left([B_0] + \frac{1}{2}[B_L]\right)\{d\}. \tag{9}$$

Where $[B_0]$ contains the linear terms of eq. (11), while $[B_L]$ comprises its quadratic contributions.

4 Tangent stiffness matrix

The tangent stiffness matrix governs the equilibrium iterations and reflects the structure's current configuration. It comprises two components: the large displacement stiffness matrix K_L, includes both elastic and nonlinear effects, and the geometric stiffness matrix K_σ, which accounts for stiffness induced by axial forces in the deformed state, as shown in Vasilescu [7]. Based on the Principle of Virtual Work, it can be expressed as:

$$K_T = K_L + K_\sigma = \int_V [B]^T [D][B] dV + \int_V [G]^T \{\sigma\}[G] dV. \tag{10}$$

Where $[D]$ is the constitutive matrix, $[G]$ the gradient matrix associated with the kinematic displacement vector (see eq. (6)), and $\{\sigma\}$ the stress vector.

Since this nonlinear system cannot be solved directly, incremental–iterative strategies are required. According to Silva and Horowitz [8], common approaches include the Newton-Raphson method (in its full or modified form) and quasi-Newton methods. In this work, the arc-length method was employed.

5 Numerical examples

The following examples were analyzed using SimuFrame, a Python-based tool developed by the author for nonlinear structural analysis of space frames using the von Kármán model.

5.1 Simply supported beam under uniform vertical load

Before addressing space frames, the formulation is verified on a planar beam from Figueiras [5]. This step serves to clearly validate the model's core capacity for handling geometric nonlinearity. The beam (L = 6.0 m, h = 0.12 m, E = 2500 kN/m², v = 0.3) under a uniformly distributed load of 0.2168 kN/m is shown in Figure 2, with results in Figure 3.

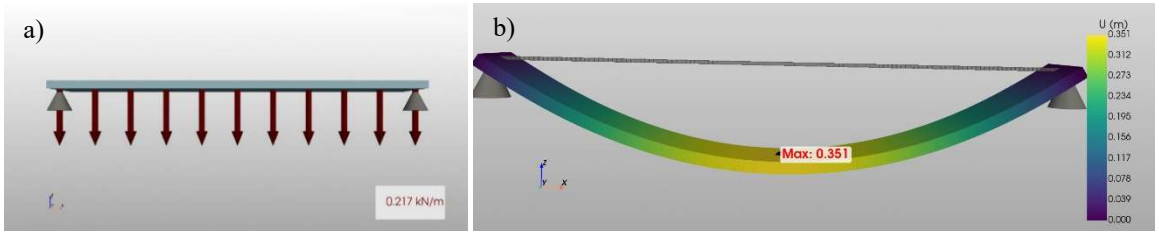


Figure 2. Simply supported beam a) undeformed and b) deformed

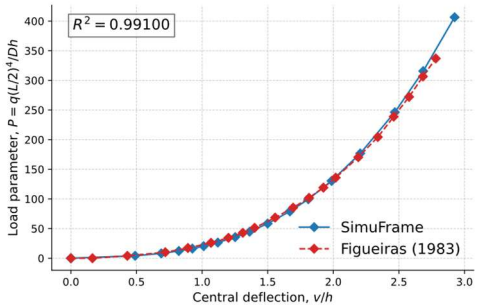


Figure 3. Load-deflection curves for simply supported beam example

For the beam benchmark, the calculated equilibrium path closely matched the reference solution, yielding a coefficient of determination (R^2) of 0.99 and confirming the model's precision in capturing nonlinear behavior.

5.2 Space frames

Two space frame examples demonstrate the software's capability. The first is an L-shaped frame with fixed ends, composed of two 4.0 m members (0.1 x 0.1 m square section; E = 200 MPa, ν = 0.2) and subjected to a 10 kN perpendicular point load (Figure 4a). The second is a four-story building designed for large-scale performance assessment, featuring 4.0 m columns and 5.0 m beams (0.2 x 0.4 m rectangular section; E = 27 GPa, ν = 0.2) with fixed base supports and distributed beam loads of 10 and 20 kN/m (Figure 4b).

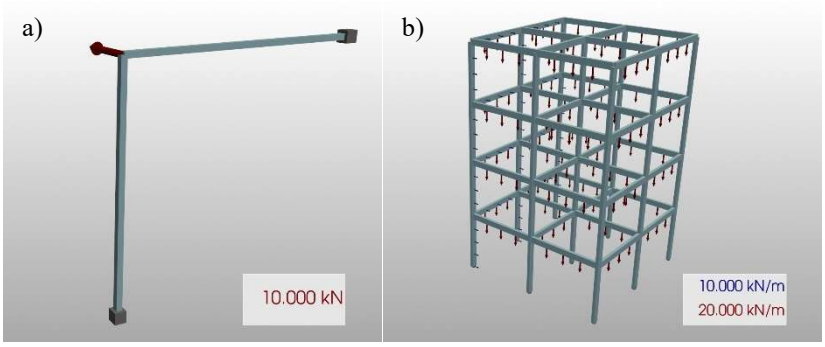


Figure 4. Structural models analyzed: a) L-shaped frame, and b) four-story building

Figure 5 compares the translations and rotations at the joint node of the L-shaped frame, where each member is discretized into 128 elements, with respect to the incremental load, computed using an arc-length algorithm, against the results obtained from Abaqus and RFEM.

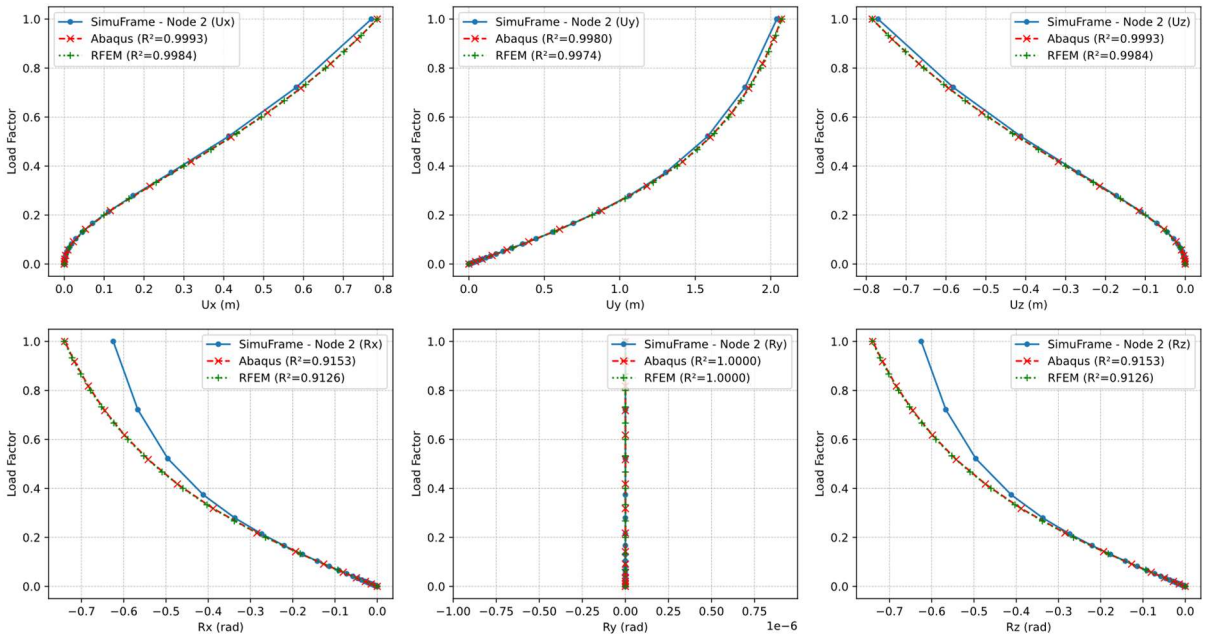


Figure 5. Comparison of equilibrium paths for the L-shaped frame at the joint node

The translations show excellent agreement with Abaqus and RFEM ($R^2 > 0.99$), while minor deviations appear in the rotations. Despite the simplifications of the von Kármán theory, the proposed tool proves suitable for practical structural design purposes, since even for deflections on the order of twice the element's height, satisfactory results are obtained.

Table 1 compares the computed load factors (λ) for the first five buckling modes of the four-story structure against reference solutions from RFEM and Abaqus.

Table 1. Load factors for the buckling analysis of the four-story space frame

Buckling mode	SimuFrame	Abaqus	RFEM
1	7.235	7.221	7.235
2	8.916	8.902	8.915
3	11.444	11.430	11.446
4	12.650	12.844	12.651
5	12.949	12.921	12.949

The minimum critical load factor shows an exact match with the RFEM results. The solution from Abaqus, while slightly more conservative in predicting lower critical loads, is also in close agreement, with a maximum deviation of only 1.5% for the fourth mode.

6 Conclusions

SimuFrame's numerical implementation demonstrated consistent accuracy across various structural systems. In the simply supported beam benchmark, its results were virtually identical to the analytical solution, validating its fundamental formulation. In the L-shaped frame analysis, the translational results showed excellent agreement with both Abaqus and RFEM, achieving a coefficient of determination exceeding 0.99.

In the buckling analysis of the four-story structure, the critical load factors matched the RFEM results exactly for all modes and remained in close agreement with Abaqus. This strong agreement with both analytical and commercial benchmarks validates the robustness of the implemented formulation for capturing complex nonlinear and stability phenomena, reinforcing the tool's potential for academic use and future development.

Acknowledgements. The authors thank the examination committee for their time and valuable feedback.

Authorship statement. The authors hereby confirm that they are the sole liable persons responsible for the authorship of this work, and that all material that has been herein included as part of the present paper is either the property (and authorship) of the authors, or has the permission of the owners to be included here.

References

[1] R. S. Lotti, A. W. Machado, Ê. T. Mazzieiro, and J. Landre Júnior, "Aplicabilidade científica do método dos elementos finitos," *Rev. Dent. Press Ortodon. Ortop. Facial*, vol. 11, pp. 35–43, 2006, doi: https://doi.org/10.1590/S1415-54192006000200006.

[2] L. E. Vaz, *Método dos Elementos Finitos em Análise de Estruturas*. Rio de Janeiro: Elsevier, 2011.

[3] O. C. Zienkiewicz, R. L. Taylor, and J. Z. Zhu, Eds., "The Finite Element Method: Its Basis and Fundamentals," in *The Finite Element Method: its Basis and Fundamentals (Seventh Edition)*, Oxford: Butterworth-Heinemann, 2013, p. i. doi: 10.1016/B978-1-85617-633-0.00019-8.

[4] E. P. Foletto, R. C. Pavan, S. E. Pilz, and M. F. Costella, "Estudo da não linearidade geométrica, instabilidade e ruptura de estruturas espaciais reticuladas," *Engevista*, vol. 21, no. 1, Art. no. 1, 2019, doi: 10.22409/engevista.v21i1.

[5] J. de A. Figueiras, "Ultimate load analysis of anisotropic and reinforced concrete plates and shells," 1983, Accessed: July 05, 2025. [Online]. Available: https://repositorio-aberto.up.pt/handle/10216/11772

[6] M. A. C. Rodrigues, R. B. Burgos, and L. F. Martha, "A unified approach to the Timoshenko 3D beam-column element tangent stiffness matrix considering higher-order terms in the strain tensor and large rotations," *International Journal of Solids and Structures*, vol. 222–223, p. 111003, July 2021, doi: 10.1016/j.ijsolstr.2021.02.014.

[7] A. Vasilescu, "Analysis of geometrically nonlinear and softening response of thin structures by a new Facet Shell Element," Thesis (Master of Civil and Environmental Engineering), Carleton University, 2000. Accessed: Nov. 23, 2024. [Online]. Available: https://hdl.handle.net/20.500.14718/35846

[8] J. R. de B. Silva and B. Horowitz, "Nonlinear analysis of reinforced concrete structures using thin flat shell elements," *Rev. IBRACON Estrut. Mater.*, vol. 15, p. e15407, Feb. 2022, doi: https://doi.org/10.1590/S1983-41952022000400007.